

The Effects of Loading History and Crack Geometry on Time-Dependent Fatigue Crack Growth at Elevated to High Temperatures

F. Ma¹, D. Lehmann¹, T. Morrison²

¹Pratt and Whitney, East Hartford, CT 06108, USA; ²AFRL/PRTT, WPAFB Dayton, OH 45433, USA

ABSTRACT

Time-dependent fatigue crack growth was investigated in detail for a high strength nickel alloy, and several significant results were found, which are not displayed in conventional fatigue crack growth tests. Under a variety of loading conditions including dwell and mission loadings at elevated to high temperatures, fatigue crack propagation and creep crack growth tests were conducted for different crack geometries. Test results show that the crack growth rate is geometry dependent, and R-Ratio dependency (a ratio of minimum loading over maximum loading) under dwell loading conditions is reverse to those observed in conventional fatigue crack growth tests. The test results demonstrate that commonly used stress intensity factor (SIF) based fracture mechanics methodologies do not fully characterize time-dependent fatigue crack growth at elevated to high temperatures. Constraint loss of fracture mechanics was tried to correlate to the effects of crack geometry and loading conditions on dwell crack growth rate. A phenomenological model was developed to include constraint effects and model predictions have demonstrated close agreement with test data.

INTRODUCTION

Gas turbine disks of advanced aircraft engines often experience composite mission loadings at elevated to high temperatures. The missions consist of a variety of loading amplitudes, loading frequencies, and loading waveforms. High temperature dwell process (sustained peak or valley loading) is a typical engine loading condition, and greatly enhances fatigue crack growth. Understanding the mechanism of time-dependent fatigue crack growth is essential to successfully develop an accurate crack growth model and design more durable engine components with improved damage tolerance.

Over the past decades, mechanisms for fatigue crack growth rate have been investigated theoretically and experimentally by numerous researchers to identify the effects of test temperatures, loading ratio (R-Ratio), test frequency, dwell time, etc. It has been observed that fatigue-creep-environment interaction plays an important role in crack initiation and growth at high temperature for engineering materials. Pairs' pioneering work [1] is the first to use a stress intensity factor range to characterize fatigue crack growth rate. Pineau [2] performed different experiments and recognized that oxidation reaction promotes intergranular creep. A fatigue-creep crack growth model was proposed by assuming that creep crack growth is the sum of pure creep crack growth and creep crack blunting. This model greatly overestimates crack growth rate. Arguing there is no creep role in

fatigue-creep-environmental crack growth, Ghonem and Zheng [3] have proposed that at elevated temperatures and under dwell loading, fatigue crack growth is the sum of pure fatigue crack growth rate and oxidation induced crack growth rate with both a function of the range in stress intensity factor. Wei and Landes [4] assume the time-dependent fatigue crack growth can be described by a superposition of pure cyclic fatigue crack growth rate and a time-dependent crack growth rate. Collecting all effects of various environmental attacks into a creep-like crack growth, multiple attempts (e.g. [5]) have been made to fit test data under different loading conditions to serve as design methodologies.

It is worth noting that each of the above tests used stress intensity factor based model development was conducted for a single crack geometry by different researchers. This inherently assumes that stress intensity factor uniquely controls the stress and strain in the crack-tip region, and hence, crack growth. Actual cracked engine component loading states and geometries are often different from the test conditions. For elastic-plastic materials, Larson and Carsson [6] have demonstrated that plastic zone and shape of the crack tip-region under small scale yielding (SSY) conditions are strongly affected by a constraint parameter. Therefore, a single stress intensity factor does not uniquely dominate stress and strain in the plastic and creep zone, and crack initiation and propagation are actually controlled by two parameters. There are several approaches [7,8,9] to define the constraint parameter. One uses elastic T-stress for the SSY problem, which represents a tensile or compressive stress acting parallel to the crack plane. The others use elastic-plastic solutions based on Q-stress or stress triaxiality A_m for general yielding problems. Considering that most fatigue crack propagation problems are under small scale yielding, and elastic analysis is easy and widely used in industry, the T-stress approach is used through this paper.

For time-dependent fatigue crack growth, in particular when dwell load is applied at elevated to high temperatures, creep and plasticity at the crack tip is no longer negligible, and stresses in the creep and plastic region are redistributed. The T-stress approach for constraint effects in elastic-plastic fracture mechanics is directly used in this paper for time-dependent fatigue crack propagation at high temperatures. Due to the homogeneous nature of the governing equations for creep crack problems, the time-dependent creep stress field in the crack tip region can be approximately regarded as a time-dependent plastic stress field [10] for time-dependent proportional loading.

In this paper, several significant results observed from time-dependent crack growth tests will be provided first, followed by a discussion of the effects of crack geometry and loading conditions in fracture mechanics. Then variation of constraint with test specimen geometries and loading conditions will be tried to correlate to the phenomenon observed from time-dependent fatigue crack growth tests. Finally, a phenomenological model is developed and will be used to predict time-dependent fatigue crack growth in different specimens and under different loading conditions.

TEST AND RESULTS

In order to understand the effects of test temperature, loading ratio (R-Ratio), test frequency and dwell time, the test program focused on two kinds of crack growth tests with environment attacks. One is for dwell fatigue crack growth and the other is for time-dependent creep crack growth. Conventional fatigue crack growth is a special case for time-dependent fatigue crack growth, and results from available conventional fatigue crack growth test data and models were used to support the methodology development. However, since numerous tests on conventional fatigue crack propagation (with high frequency loading and with out hold-time at peak or valley loading) are commonly available, no additional conventional fatigue crack growth testing was conducted.

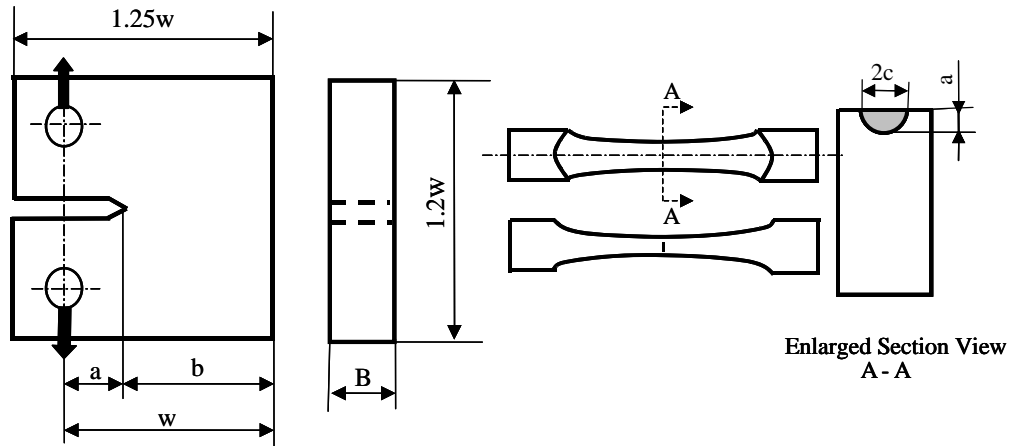


Figure 1. Compact Tension (CT) and Surface Flaw (SF).

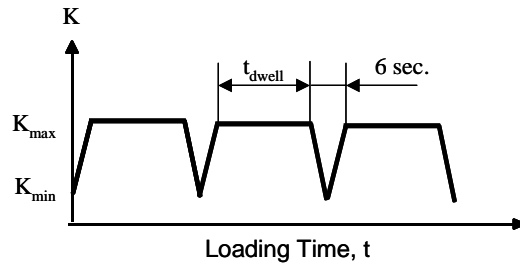


Figure 2. Characteristics of 2-minute dwell loading history

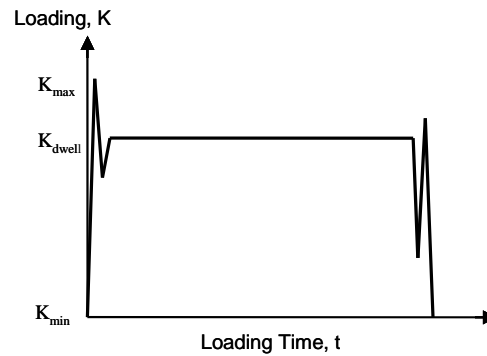


Figure 3. Characteristics of a mission loading history

Test Specimens

Two different fracture specimens, compact tension (CT) and surface flaw (SF), were used to account for the effects of crack geometry on time-dependent crack growth. The compact tension (CT) specimen, which is an ASTM recommended geometry for fracture testing, can provide conservative test data for use in assessing different crack geometries and cracked components. The surface flaw (SF) specimen is representative of most actual cracks in engineering applications. The crack is initiated as an approximate semi-circle on the specimen surface and is subjected to remote uniform tensile loading. The geometries for both specimens are showed in Figure 1.

Loading History

Loading was measured by the elastic stress intensity factor, K . A 2-minute dwell loading was used to account for the effects of hold time on fatigue crack growth. The loading was increased from a minimum loading, K_{\min} , to a maximum loading, K_{\max} , in 3 seconds, followed by 2-minute constant loading. Then the loading was reduced to minimum again in 3 seconds. The cycle was repeated and crack growth rate was measured against the loading history. The loading profile is displayed in Figure 2. The loading profile is characterized by R-ratio, $R = K_{\min} / K_{\max}$, and stress intensity factor range, $\Delta K = K_{\max} - K_{\min}$. In this test program, two R-ratios were run, $R=0.1$ and 0.3 , to account for the effects of mean loading on time-dependent fatigue crack growth.

Creep crack growth tests were run to measure crack growth change with time at a given loading. To obtain creep crack growth rates at different loading levels, a fatigue crack growth approach with $R=1$ was used. The loading was characterized by the maximum loading in term of K .

In order to consider the effects of over loading on dwell crack growth, a test was run with a CT specimen under a simple mission loading. The mission loading consists of an over-load, a 2-minute dwell load and 2 sub-cycle loadings. The details of the mission loading are displayed in Figure 3. The minimum loading for this mission was zero, resulting in an R-ratio of zero with the stress intensity factor range equal to the maximum stress intensity factor, $\Delta K = K_{\max}$.

Dwell Fatigue Crack Growth Test Results

Dwell fatigue crack growth rate was measured and plotted versus stress intensity range, ΔK , at different temperatures. There are several findings from these tests, which are significantly different from results of conventional fatigue crack growth tests, demonstrating that single stress intensity factor alone is not enough to characterize time-dependent fatigue crack growth.

Included in Figure 4 are the results for the CT specimens at $R=0.1$. At elevated temperatures, it was found that applied dwell loading accelerates the Region II fatigue crack growth rate relative to the conventional fatigue crack growth rate. However, it seems the threshold does not change significantly at elevated

temperatures. At higher temperatures, the dwell crack growth rate is slower than conventional fatigue crack growth rate for loading close to the threshold value.

In conventional fatigue crack growth tests, it is widely accepted that increasing the mean loading results in an increase in crack growth rate. But this was not observed in the dwell crack growth testing. Displayed in Figure 5 are the CT specimen dwell test results at $R=0.1$ and $R=0.3$. Clearly, at higher temperatures the crack growth rate is slower at $R=0.3$ than at $R=0.1$. When the temperature is reduced to 1100°F , the two R-ratio results are almost identical.

It can be concluded from the results in Figures 4 and 5 that there is a critical temperature (around 1000°F) for the onset of creep and environmental attacks. For temperatures less than the critical value, the effects of creep and environment are not evident. It is expected that when temperature is reduced further, the effects of R-ratio will follow those for conventional fatigue tests.

Crack geometry effects can be significant on fatigue crack growth under dwell loading. Figure 6 displays the dwell test results from both CT and SF specimens under the same test conditions. Tests were run at two temperatures, 1200°F and 1300°F . At both temperatures the crack growth rate was faster in the CT specimens than in the SF specimens even though the same loading was applied, demonstrating that a single parameter K based fracture mechanics methodology is unable to characterize the geometry effect. This effect is not evident in conventional fatigue crack growth testing. For the 1300°F SF specimen test, a step change in the crack growth rate was observed. This test was restarted on a second day after being held at 1300°F overnight at low load. It is anticipated that the high temperature low load dwell resulted in a redistribution of the stresses around the crack tip and a subsequent reduction in the crack growth rate. Additional testing is warranted to further investigate this observation.

Creep Crack Growth Rate

In order to separate out the contribution of creep and environmental attack versus the cyclic contribution to crack growth under dwell loading, creep crack growth tests were conducted for CT specimens at multiple temperatures. Creep crack growth rates at the different temperatures are plotted against the loading in term of stress intensity factor in Figure 7. As expected, the creep crack growth rate accelerates as loading and temperature increase. It is noted that environmental attack is expected to have the same effect for the creep crack growth and the cyclic dwell crack growth tests at the same exposure time, loading level and temperature.

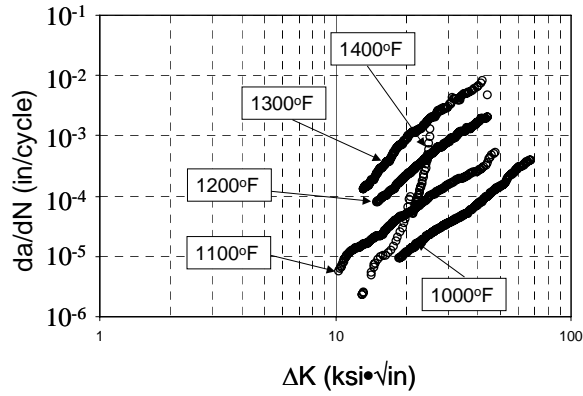


Figure 4. Dwell crack growth rates da/dN in CT specimen, $R=0.1$.

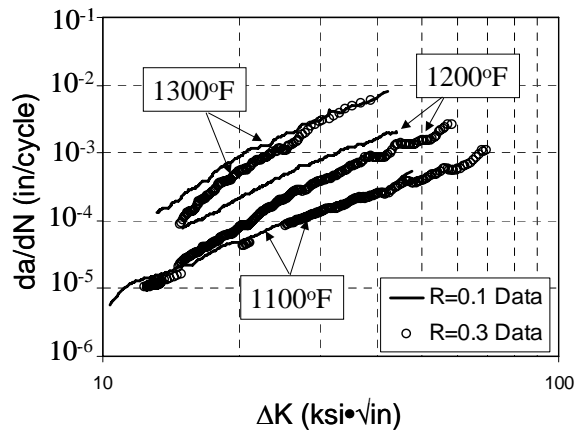


Figure 5. Dwell crack growth rates da/dN at in CT specimen, $R=0.1$ and 0.3 .

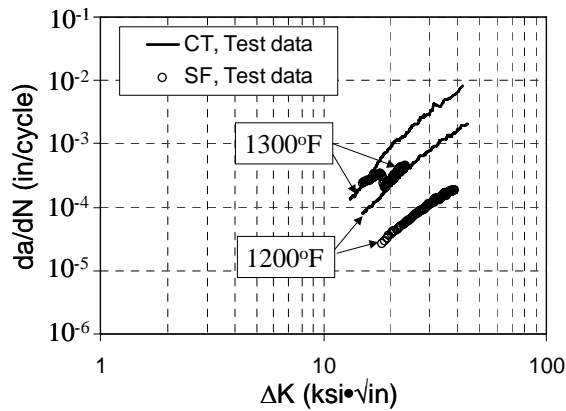


Figure 6. Dwell crack growth rates da/dN for CT and SF specimens, $R=0.1$.

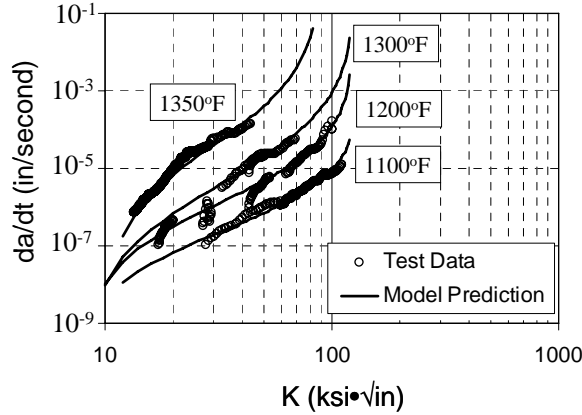


Figure 7. Creep crack growth rates da/dt for CT specimens

TIME-DEPENDENT FATIGUE CRACK GROWTH MODEL

An attempt has been made to demonstrate that the effects of constraint on fracture mechanics can be correlated to the phenomenon observed from time-dependent fatigue crack growth tests. A phenomenological model for crack growth with environment assisted creep interaction has been developed. First, the fundamental concepts of constraint loss in fracture mechanics are presented, and an appropriate crack propagation driving force is defined. Then, a time-dependent crack growth rate model is formulated. Dwell crack growth is a special case for this model.

Constraint Loss of Fracture Mechanics

Fracture mechanics theory provides a strong tool for fatigue crack growth characterization. Over the past few decades, advances in constraint treatment of fracture mechanics have been achieved. Various approaches have been proposed to characterize the constraint loss associated with fracture mechanics. In particular for fatigue crack problems, the stress in the crack-tip is approximated as an SSY problem. Elastic stress fields in the crack-tip region are characterized as a function of stress intensity factor, K , and T-stress, T_s [11],

$$\sigma_{ij} = \frac{K}{\sqrt{2\pi r}} f_{ij}(\theta) + \delta_{i1} \delta_{1j} T_s \quad (1)$$

where, r and θ are polar coordinates with the origin at crack tip; $\theta=0$ is the crack growth direction; and $f_{ij}(\theta)$ is a universal function.

As discussed in the introduction section, T-stress significantly affects the plastic and creep zone size and shape. The elastic-plastic stresses are characterized by O'Down and Shih [8] using a J-integral and Q-stress as ,

$$\frac{\sigma_{ij}}{\sigma_y} = \left(\frac{J}{\alpha \epsilon_y \sigma_y I_n r} \right)^{\frac{1}{n+1}} \hat{\sigma}_{ij} + \delta_{ij} Q. \quad (2)$$

Where, σ_y and ε_y are the yield stress and strain, respectively, and α and $n > 1$ are Ramberg-Osgood material strain hardening constants. I_n and $\sigma_{ij}(\theta, n)$ are universal functions of the hardening exponent n .

From equation. 2, an equivalent J-value can be defined using the same tensile stress, σ_c , in the crack-tip region,

$$J_{eq} = J \left(1 - \frac{\sigma_y}{\sigma_c} Q \right)^{-(n+1)}. \quad (3)$$

For SSY problems, the J -integral can be related to stress intensity factor, K , and Q -stress to T -stress [12], $Q = Q(T_s)$. Therefore, an equivalent K from equation. 3 is,

$$K_{eq} = K \left(1 - \frac{\sigma_y}{\sigma_c} Q(T_s) \right)^{-\frac{n+1}{2}}. \quad (4)$$

The fracture condition can be expressed as

$$K_{eq} = K_{IC}, \quad (5)$$

where K_{IC} is a material constant under high constraint condition ($Q=0$). This can be tested by using ASTM recommended standard specimen. Thus K_{eq} plays the same role as K does in single parameter fracture mechanics. The constraint effects on crack initiation and propagation can be addressed by an equivalent crack driving force.

The equations above can be rewritten as

$$K = K_{IC} A_T, \quad (6)$$

where

$$A_T = \left(1 - \frac{\sigma_y}{\sigma_c} Q(T_s) \right)^{\frac{n+1}{2}}. \quad (7)$$

Thus, K is still used as the crack driving force, but material resistance for crack propagation must be characterized by an equivalent crack propagation resistance, $K_{IC} A_T$.

Time-Dependent Fatigue Crack Growth Model

As discussed previously, crack initiation and propagation depend on both the stress intensity factor, K , and constraint level characterized by T -stress. Instead of doing rigorous calculations for T -stress, the general tendency of constraint change with crack geometry and loading was used to demonstrate that constraint concepts can successfully characterize the phenomenon observed in time-dependent crack growth tests, which can not be explained using the K -dominated fracture mechanics knowledge.

Time-dependent fatigue crack growth is accelerated by environmental attacks and creep damage. Environmental attacks play a very important role in the

acceleration of crack growth. This was accounted for through the material constants in the creep crack growth model, because creep testing was performed in the same environmental conditions as time-dependent crack growth. Creep develops time-dependent plasticity in the crack-tip region, resulting in a change of constraint, and a reduction in the crack growth rate.

For cyclic loading it is assumed that the constraint does not change significantly during unloading. Using published results of T-stress in [12,13] for different specimens, T-stress under cyclic loading is approximated as,

$$T_s \approx -\tau \frac{\Delta K}{\sqrt{\pi a}}; \quad (8)$$

where $\tau=3/9$ for a CT specimen at $R=0.1$, and $\tau=3/7$ for a CT specimen at $R=0.3$. For an SF specimen, $\tau=8/9$ at $R=0.1$.

As analyzed in equation. 7 previously, negative T-stress reduces the crack driving force, or increases material resistance for crack propagation. Comparing T-stresses at $R=0.1$ and $R=0.3$ for CT specimens, it is found that the negative T-stress at $R=0.1$ is smaller than at $R=0.3$, i.e. T-stress reduces crack growth more at $R=0.3$ than at $R=0.1$. On the other hand, because negative T-stress is larger in an SF than in a CT specimen, it reduces crack growth rate more in the SF than in the CT specimen. This is the tendency observed in the dwell crack growth tests.

Thus, a time dependent crack growth model using the concepts of fracture mechanics can be developed. It includes fatigue, creep and environment interactions. The increment of crack growth within a time increment, dt , is assumed to result from pure fatigue crack growth and environment assisted creep crack growth,

$$da = da_F + da_C; \quad (9)$$

where da_F represents a pure time-independent fatigue crack increment caused by cyclic loading only. da_C is the increment due to environment assisted creep damage. It depends on loading history, because both environmental attack and creep are time dependent processes. Equation (9), in general, is expressed in the form of fatigue crack growth rate by integration over a loading cycle,

$$\frac{da}{dN} = \frac{da}{dN}\bigg|_F + \frac{da}{dN}\bigg|_C. \quad (10)$$

The two parts will be discussed in further detail.

Fatigue Crack Growth Model

Because of the common acceptance of the Paris law in characterization of region-II fatigue crack growth, Priddle [14] modified the Paris law to include the effects of crack initiation and unsteady processes

$$\frac{da}{dN}\bigg|_F = C \left(\frac{\Delta K - \Delta K_{th}}{K_c - K_{max}} \right)^m, \quad (11)$$

where C and m are material constants and ΔK_{th} is the threshold stress intensity factor for fatigue crack growth. Threshold and critical stress intensity factors represent two limit cases for fatigue crack growth.

It is noted that the model assumes that K is the crack driving force but does not account for the effects of crack closure and constraint loss. Crack closure is due to accumulated plasticity in the crack-tip region. It can be expected that the effort for a higher loading is small relative to the effect for a lower loading [15]. Therefore, the closure effect on fatigue crack propagation is accounted for through its effect on the threshold; i.e. threshold ΔK_{th} is replaced by $f(R)\Delta K_{th}$, and $f(R)$ is a function of R-ratio. Thus fatigue crack growth in equation.11 becomes

$$\left. \frac{da}{dN} \right|_F = C \left(\frac{\Delta K - A_T^{th} \cdot f(R) \cdot \Delta K_{th}}{A_T^c \cdot K_c - K_{max}} \right)^m, \quad (12)$$

where A_T^{th} and A_T^c represent constraint effects, calculated by Equations.(6,7 at threshold and unsteady crack propagation loadings, respectively.

Environmentally Assisted Creep Crack Growth

Creep crack growth rate is a function of the crack driving force. Experimental data shows that once the loading reaches a critical loading, K_c , the crack starts to unsteadily propagate, and when loading is less than another special value, K_{th}^c , crack growth will not initiate. This value is referred to as the threshold for creep crack growth. Like fatigue crack growth, the equivalent crack propagation resistance is used for threshold and unsteady crack propagation. Pure creep crack growth rate is expressed as

$$\frac{da}{dt} = b \left(\frac{K - A_T^{th} \cdot K_{th}^c}{A_T^c \cdot K_c - K} \right)^q, \quad (13)$$

where b and q are temperature dependent material constants.

It is noted that the effects of environmental attacks on creep crack propagation have been included through material constants in this model. The material constants change with test environment, e.g. in air and in vacuum.

Time-dependent loading is different from pure creep loading. Relative to pure creep crack propagation, the cyclic loading (fatigue) in time-dependent loading damages the material ahead of the creep crack-tip, so the creep crack propagation rate associated with cyclic loading is faster than the pure creep crack growth rate in equation. 13. To account for the interaction, an interaction factor, η , is introduced to characterize environmentally assisted creep crack growth under time-dependent loading conditions,

$$\frac{da}{dt} = b \left(\eta \cdot \frac{K - A_T^{th} \cdot K_{th}^c}{A_T^c \cdot K_c - K} \right)^q. \quad (14)$$

3.5 Time-Dependent Crack Growth Model

With the creep and fatigue crack growth models developed; the time-dependent crack growth model is obtained by substituting equation.12 and 14 into equation.10,

$$\frac{da}{dN} = C \left(\frac{\Delta K_{eff} - A_T^{th} \cdot f(R) \Delta K_{th}}{A_T^c K_c - K_{max}} \right)^m + \int a \left(\eta \frac{K_{max} - A_T^{th} \cdot K_{th}^c}{A_T^c \cdot K_c - K_{max}} \right)^b \cdot dt \quad (15)$$

For time-dependent loading, the second part on the right hand of equation.15 is loading history dependent. For example, for the same loading waveform, the crack growth rate is increased with decreasing frequency. When loading frequency is given, a different loading profile will lead to a different crack growth rate.

In particular, for dwell crack growth, loading held for a period, t_{dwell} , at maximum loading is approximately taken as constant over the loading cycle and the crack growth rate is

$$\frac{da}{dN} = C \left(\frac{\Delta K_{eff} - A_T^{th} \cdot f(R) \Delta K_{th}}{A_T^c \cdot K_c - K_{max}} \right)^m + a \left(\eta \frac{K_{max} - A_T^{th} \cdot K_{th}^c}{A_T^c \cdot K_c - K_{max}} \right)^b t_{dwell} \cdot \quad (16)$$

MODEL PREDICTION AND DISCUSSION

With the time-dependent fatigue crack growth models developed previously, the material constants in the model are identified by a combination of pure fatigue crack growth tests, creep crack growth tests, and dwell crack growth data.

In rest of this paper, the crack growth model will be applied to different test cases. Stress intensity factors are calculated using the formula in reference [12]. Using the published T-stress [12,13] for various specimens as a guide, A_T is estimated for the CT and SF specimens used in this work at threshold loading and fracture toughness loading.

First, the fatigue crack growth model in Equation.12 is identified using the test data under high frequency loading (10cpm). Because loading frequency is high, creep does not play a big role in crack propagation and constraint effects are ignored, i.e. $A_T=1$. Material constants, C and m are identified by 10 cpm crack growth test data, and are directly used in the dwell crack growth model, Equation. 16.

Creep Crack Growth

The creep crack growth model in Equation.14 is used to predict the creep crack growth for CT specimens at different temperatures ranging from 1100°F to 1350°F. The creep fatigue interaction factor for this specimen is taken as unity, $\eta=1$. Because at lower loading the CT has a constraint level closer to that for single parameter crack-tip fields than for CT with $R=0.3$, and for SF, the T-stress is approximated to zero for CT specimens for creep and $R=0.1$ dwell crack

growth. From Equation.7, $A_T=1$ for this case. Using $A_T=1$ and $\eta=1$ in Equation. 14, it is found that the model characterizes creep crack growth very well as shown in Figure 7 for the CT specimen.

Dwell Crack Growth in CT

A single parameter fracture mechanics methodology ($T_s=0$, and $A_T=1$) is used for the CT specimen at $R=0.1$ as discussed before. Similarly, crack closure effects are ignored at $R=0.1$ relative to the other tests, $f(R)=1$. By comparison of the dwell test data to creep and fatigue crack growth rate, the creep fatigue interaction factor is found to be $\eta=2.3$. Using the values in Equation.16, the model can predict crack growth rate well compared with test data as shown in Figure 8.

As R-ratio increases, maximum loading is increased, creep and plasticity are developed in the crack tip region, and constraint and crack closure take effect. In Equation. 7, A_T is increased, and $f(R)$ is taken approximately as 0.87. It is found that by accounting for an increased A_T value, the model gives a very good prediction for test data as illustrated in Figure 9.

Dwell Crack Growth for SF

For the surface Flaw (SF) specimen, stress and strain fields in the crack tip region deviate from single fracture parameter characterization even for low loading [14]. When applying the constraint effects in Equation. 7 to the dwell crack growth model, the model predictions match the test data well as displayed in Figure 10.

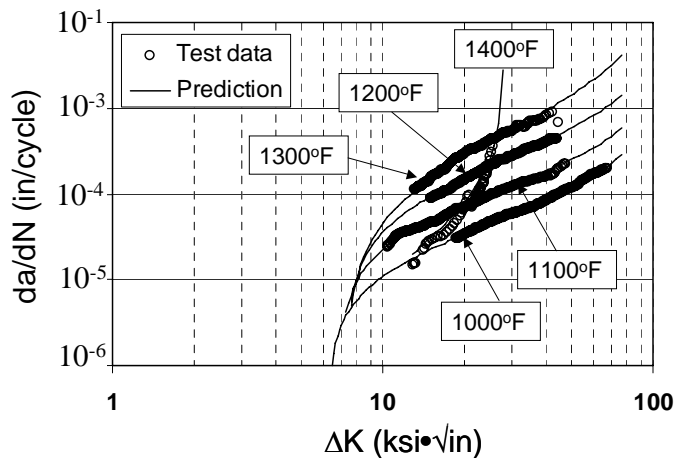


Figure 8. Comparison of dwell crack growth rate data and model characterization for CT specimens at $R=0.1$.

Mission Validation Testing

Under mission loading, the fatigue crack growth rate was measured against the stress intensity factor range. This result was used to verify the life model developed from dwell and creep tests data.

For the applied mission loading (Figure 3), dwell and sub-cycle loadings are under elastic deformation conditions. The initial over-loading produces a large plastic strain and hardens the material (increases flow stress), resulting in retardation of crack advance for the dwell and sub-cycle loadings. Therefore, the mission loading can be regarded as an $R=0$ loading with maximum loading equal to K_{max} in this mission, and creep crack growth part in the dwell crack growth model is ignored, and the constraint interaction factor is taken as unity as used for $R=0.1$. As shown in Figure 11, the crack growth rate is predicted well by the fatigue crack growth model with $f(R) = 1.6$.

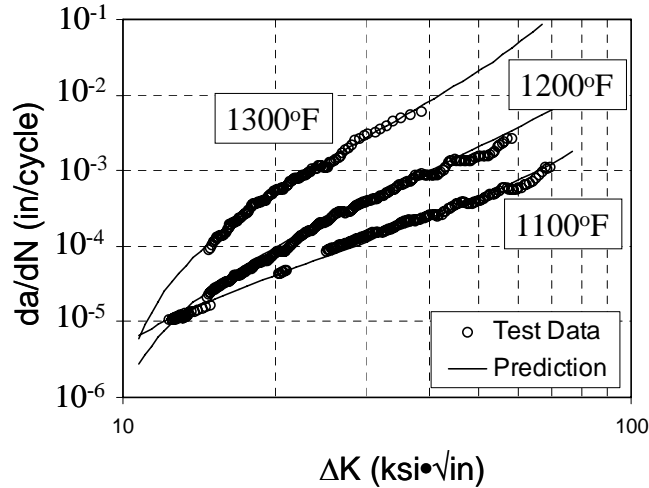


Figure 9. Comparison of dwell crack growth rate data and model characterization for CT specimens at $R=0.3$.

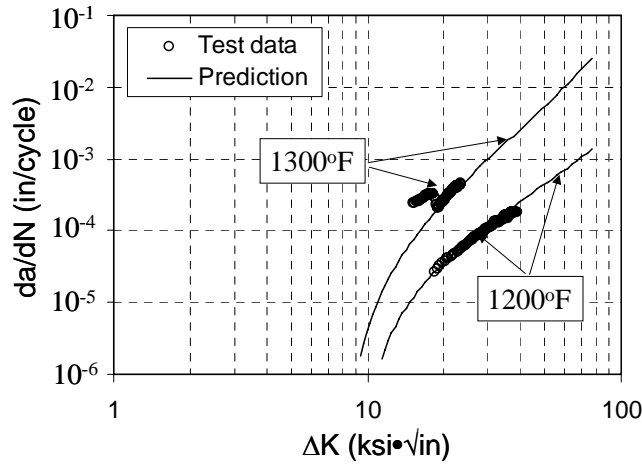


Figure 10. Comparison of dwell crack growth rate data and model characterization for SF specimens at $R=0.1$.

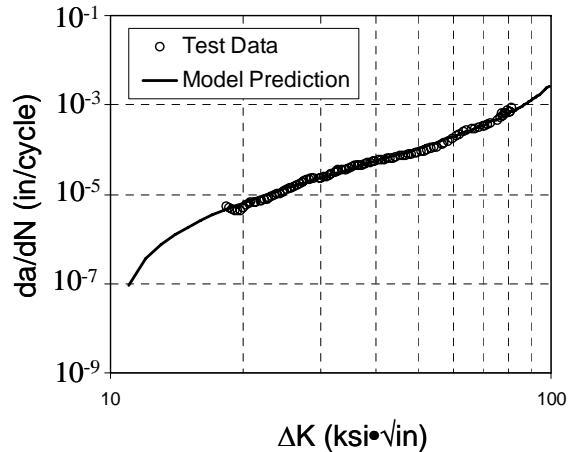


Figure 11. Crack growth rates da/dN in CT under mission loading, $T=1200^{\circ}\text{F}$.

CONCLUDING REMARKS

Time-dependent fatigue crack growth was experimentally investigated in detail for a high strength nickel alloy. Test data showed that crack growth rate is much faster in a CT specimen than in SF for same dwell test condition. This behavior is not evident in conventional fatigue crack growth testing. R-ratio dependence of the crack growth rate follows a reversed trend relative to that observed from conventional fatigue crack growth testing.

The test results demonstrate that a single-parameter fracture mechanics methodology is unable to fully characterize time-dependent crack growth at elevated to high temperatures. Constraint loss of fracture mechanics may be the reason for the phenomenon observed from the time-dependent crack growth tests. The constraint variation in different geometries and at different loading is consistent with the crack growth rate variation for different specimens and loadings.

The results of the model development effort are very promising if constraint effects are accounted for in the characterization of time-dependent crack propagation. Further, analysis is recommended in this field of study to continue to develop a detailed understanding of the constrain change and further develop these physical based time-dependent crack growth models.

ACKNOWLEDGMENTS

The authors would like to thank Dr Rick Pettit for his valuable comments and suggestions, and Mr. Brent Barber who performed all of tests reported.

REFERENCES

- [1] P. Pairs, P. F. Erdogan, (1963) A critical analysis of crack propagation laws, *J. Basic Engineering*, 85 (1963) 528-534.
- [2] A. Pineau, Intergranular creep-fatigue crack growth in Ni-Base Alloys, *Flow and Fracture at Elevated Temperatures* (edited by R. Raj) Metals Park, Ohio 44073. American Society for Metals. (1985) 317-348.
- [3] H. Ghonem, D. Zheng, Depth of intergranular oxygen diffusion during environment dependent fatigue crack growth in alloy 718, *Materials Science and Engineering* 150A (1992)151-160.
- [4] R. P. Wei, J. D. Landes, Correlation between sustained load and fatigue crack growth in high-strength steels, *Mater. Res. Stand.*, 9(7) (1969) 25-28.
- [5] R. H. VanStone, O.C. Gooden, D. D. Krueger, A final report of Advanced Cumulate Damage Modeling, GE Aircraft Engines, Cincinnati, Ohio 45215, 1988.
- [6] S. G. Larson, A. J. Carsson, Influence of non-singular stress terms and specimen geometry on small-scale yielding at crack-tip in elastic-plastic materials, *J. Mech. Phys. Solids*, 21 (1973) 263-278.
- [7] C. Betegon, J. W. Hancock, Two-parameter characterization of elastic-plastic crack –tip fields, *ASME J. Appl. Mech.*, 58 (1991) 104-110.
- [8] N. P. O’Dowd, C. F. Shih, Family of crack-tip fields Characterized by a Triaxiality parameter, *J. Mech. Phys. Solids*, 39 (1991) 989-1015.
- [9] F. Ma, M. A. Sutton, X. Deng, Plane strain mixed crack-tip stress fields characterized by a triaxial stress parameter and a plastic deformation extent base characteric length, *J. Mech. Phys. Solids*, 49 (2001) 2921-2953.
- [10] M. F. Kanninen, C. H. Popelar, *Advanced Fracture Mechanics*, Oxford University Press, New York, 1985
- [11] M. L. Williams, On the stress distribution at the base of a stationary crack, *ASME J. Appl. Mech.* 24 (1957) 109-114.
- [12] T. L. Anderson, *Fracture Mechanics: Fundamentals and Applications*, Second Edition, CRC Press, 1994
- [13] X. Yu, X. Wang, Weight functions for T-stress for semi-elliptical surface cracks in finite thickness plates, *J. Strain Analysis*, 40 (2005) 1-17.
- [14] E. K. Priddle, High cycle fatigue crack propagation under random and stantantamplitude loadings, *Int. J. Pressure Vessels and Piping*, 4 (1976) 89-117.
- [15] W. Elber, Fatigue crack closure under cyclic tension, *Engng. Fract. Mech.*, 2 (1970) 37-45.